Preprint
UCRL-ABS-203979

Symbolic Implicit Monte Carlo radiation transport in the difference formulation: a piecewise constant discretization

Eugene D. Brooks III, Michael Scott McKinley, Frank Daffin, Abraham Szoke

This article was submitted to Elsevier Science

U.S. Department of Energy

Lawrence Livermore National Laboratory

19 April 2004

Approved for public release; further dissemination unlimited

DISCLAIMER

This document was prepared as an account of work sponsored by an agency of the United States Government. Neither the United States Government nor the University of California nor any of their employees, makes any warranty, express or implied, or assumes any legal liability or responsibility for the accuracy, completeness, or usefulness of any information, apparatus, product, or process disclosed, or represents that its use would not infringe privately owned rights. Reference herein to any specific commercial product, process, or service by trade name, trademark, manufacturer, or otherwise, does not necessarily constitute or imply its endorsement, recommendation, or favoring by the United States Government or the University of California. The views and opinions of authors expressed herein do not necessarily state or reflect those of the United States Government or the University of California, and shall not be used for advertising or product endorsement purposes.

This is a preprint of a paper intended for publication in a journal or proceedings. Since changes may be made before publication, this preprint is made available with the understanding that it will not be cited or reproduced without the permission of the author.

Symbolic Implicit Monte Carlo radiation transport in the difference formulation: a piecewise constant discretization ⋆

Eugene D. Brooks III, * Michael Scott McKinley, Frank Daffin, Abraham Szőke

University of California, Lawrence Livermore National Laboratory, P.O. Box 808, Livermore, CA 94550, USA

Abstract

The equations of radiation transport for thermal photons are notoriously difficult to solve in thick media without resorting to asymptotic approximations such as the diffusion limit. One source of this difficulty is that in thick, absorbing media, thermal emission is almost completely balanced by strong absorption. A new formulation for thermal radiation transport, called the difference formulation, was recently introduced in order to remove the stiff balance between emission and absorption. In the new formulation, thermal emission is replaced by derivative terms that become small in thick media. It was proposed that the difficulties of solving the transport equation in thick media would be ameliorated by the difference formulation, while preserving full rigor and accuracy of the transport solution in the streaming limit. In this paper, the transport equation is solved by the Symbolic Implicit Monte Carlo method and comparisons are made between the standard formulation and the difference formulation. The method was easily adapted to the derivative source terms of the difference formulation, and a remarkable reduction in noise was obtained when the difference formulation is applied to problems involving thick media.

Key words: difference formulation, radiation transport, implicit Monte Carlo

⋆ This work was performed under the auspices of the U.S. Department of Energy by the University of California, Lawrence Livermore National Laboratory under contract No. W-7405-Eng-48.

* Corresponding Author:
Email address: brooks3@llnl.gov (Eugene D. Brooks III,).

1 Introduction

The transport of thermal photons in thick media is of sufficient importance that substantial effort has been expended in developing both deterministic [1–4] and Monte Carlo [5] methods for its solution. The difficulties associated with thick media have been severe enough to necessitate solving asymptotic approximations, such as the Eddington and diffusion approximations [6], instead of solving the full transport equation.

Asymptotic methods do give the right solution to the transport equation in uniformly thick media, like stellar interiors. Nevertheless, in many problems of interest the medium is a mixture of thick and thin regions; moreover, some regions of interest may be thin for some radiation frequencies and thick for others.

Although a lot of progress has been made in numerical calculations for such complicated systems using asymptotic methods, they suffer from several defects. One such defect is an unphysical energy propagation rate when the method is applied outside its proper domain. This led to the development of *ad hoc* corrections such as flux limiters [7]. Another defect is that asymptotic methods are unable to satisfy correct boundary conditions. Time honored "fixes" are the Marshak [8] and Mark [9] boundary conditions, but these incorrect boundary conditions distort ubiquitous boundary layers. More importantly, it is difficult to estimate or measure the errors incurred by the approximations. Only an accurate solution of the transport equation is able to eliminate the above defects.

Several hurdles have stood in the way of producing accurate Monte Carlo solutions of the transport equation in thick media. The first is the selection of a Monte Carlo technique that is numerically stable and provides correct treatment of the stiff coupling between the radiation and the material in the thick limit. Several authors have shown that the radiation matter coupling is properly treated by the Symbolic Implicit Monte Carlo method (SIMC) [10,11], producing a correct implicit solution of the radiation field and the material temperature at the end of a time step [12], while effective scattering techniques [5,13,14] possess a significant deficiency in this regard.

A second hurdle has been the very significant noise problem, or the equivalent problem of computational efficiency, when Monte Carlo methods are pressed into service for thick systems. The energy is emitted in a zone uniformly, but only particles born within a few mean free paths of a zone boundary have any chance of contributing to the flux across the boundary. Most of the emitted particles are absorbed within the same zone and serve only to compute the equilibrium values of the radiation intensity and temperature in

that zone. This situation for the Monte Carlo method, as applied to thermal photon transport, has been a source of frustration for a long time. The local equilibrium value of the radiation intensity in the thick limit is, of course, the black-body field for the given local temperature. One would prefer not to waste a lot of processing power computing it.

In earlier work [16], some of the authors proposed a new formulation for the transport of thermal photons, referred to as the *difference formulation*. In this scheme, the transport equation is transformed by considering a new field that is the deviation of the local intensity from the local equilibrium intensity. The result of the transformation is to remove the thermal emission source from the transport equation, replacing it with derivative sources that are small in the thick limit. A reasonable conjecture would be that, in the Monte Carlo solution for the transport of the difference field, a significant gain in the noise figure would result.

In this paper, we demonstrate the validity of this conjecture for the transport of thermal photons. We find that, by employing the difference formulation in a Monte Carlo environment, the effective gain in computational efficiency as compared to the standard formulation increases quadratically with the optical thickness of the problem. This advantage in computational efficiency appears in all portions of a problem where the temperature varies relatively smoothly in space and time and, thereby, the smallness of the source terms is preserved. We describe our Monte Carlo implementation in slab geometry, comparing the implementation, accuracy and performance for the two formulations for transport.

In optically thick regions, numerical transport methods are usually applied with zone sizes that are much larger than the mean free path of a photon. A low-order discretization, that keeps the temperature and the opacity of the medium constant in each cell, does not yield the correct diffusion limit under such conditions. This "teleportation" effect was discussed in a previous paper [14]. Its deleterious effect can be reduced by using a heurisitic known as tilting [15]. Methods that produce a self-consistent solution in the diffusion limit have generated significant interest in recent years. Deterministic transport techniques which have the diffusion limit [17,18] necessarily go beyond the approximation where the zones have constant values of density, opacity and temperature. In this paper, we restrict ourselves to piecewise constant treatment of the material temperature and therefore we would *not* obtain the proper diffusion limit if the zone sizes were much larger than the photon mean free path. In the present paper we use fine zones and sidestep the issue. We intend to address this deficiency in future work using the methods of [19].

The rest of this paper is organized as follows: In Sections 2 and 3 we briefly review both the standard and the difference formulation for thermal photon

transport in slab geometry, without scattering. A more detailed description of the difference formulation, including scattering, can be found in [16]. In Section 4 we describe the SIMC method employed with a focus on how the implementation differs for the two formulations of transport. Correct frequency sampling of the source terms in the difference formulation requires an extension of the relatively mature techniques used to sample the Planck spectrum [20]. This is discussed in the Appendix. We examine the results of test problems that serve as our basis of comparison for the two transport formulations in Section 5. We end with a discussion in Section 6.

2 Radiation transport in local thermodynamic equilibrium, (LTE)

We review now the time and frequency dependent transport of photons in LTE, without physical scattering, in the standard formulation as well as in the difference formulation. For simplicity we restrict the derivation to a static medium and slab geometry. Scattering is treated identically in the two formulations and we are, therefore, less interested in examining problems with scattering. We examine problems with gray opacities and, in addition, simple frequency dependent opacities where there is a precipitous drop in opacity at higher frequencies. We also consider a temperature dependent specific heat, effectively linearizing the problem, in order to compare our Monte Carlo treatment of the difference formulation to the available analytic solutions [21].

2.1 Traditional formulation

The transport equation describes the propagation of the radiation field in terms of the specific intensity, $I(\mathbf{x}, t; \nu; \mathbf{\Omega})$, where $\mathbf{x}, t$ are the space and time variables, ν is the radiation frequency and the unit vector $\mathbf{\Omega}$ points in the direction of propagation. The specific intensity is expressed, as usual, in terms of [power / (unit area $\times$ unit solid angle $\times$ unit frequency interval)]. Using polar coordinates for the direction of propagation, $\mathbf{\Omega}$, the specific intensity can be written as $I(\mathbf{x}, t; \nu; \theta, \phi)$ with the differential of the solid angle $d\mathbf{\Omega} = d\mu d\phi$, where $\mu = cos\theta$.

In slab geometry the radiation field is symmetric around the direction perpendicular to the slab, chosen as the positive x direction. The radiation field is then independent of ϕ, and we transform the remaining angular coordinate from θ to $\mu = cos\theta$, defining $I(x, t; \nu; \mu) := I(\mathbf{x}, t; \nu; cos\theta, \phi)$, assumed to be independent of ϕ.

The transport equation, in slab geometry and LTE, is then

$$\frac{1}{c}\frac{\partial I(x,t;\nu;\mu)}{\partial t} + \mu\frac{\partial I(x,t;\nu;\mu)}{\partial x} = -\sigma'_a(\nu,T(x,t))[I(x,t;\nu;\mu) - B(\nu,T(x,t))] \quad , \tag{1}$$

where $B(\nu,T)$ is the thermal (Planck) distribution at the material temperature, $T(x,t)$, and c is the speed of light. The absorption coefficient, σ'_a, is assumed to be corrected for stimulated emission. The specific intensity is related to the photon number distribution function $f(x,t;\nu;\mu)$ by

$$I(x,t;\nu;\mu) = ch\nu f(x,t;\nu;\mu) \quad , \tag{2}$$

where $h\nu$ is the photon energy. In Eq. (1), all the variables, $I, \sigma'_a,$ and B, are functions of the independent variables, $x,t;\nu;\mu$ and/or $T(x,t)$. In the following, the independent variables will mostly be suppressed.

The emission function,

$$B(\nu,T) = \frac{2h\nu^3}{c^2}\left(e^{h\nu/kT} - 1\right)^{-1} \quad , \tag{3}$$

can be expressed in terms of a "reduced" frequency distribution function, $b(\nu,T)$,

$$B(\nu,T) = \frac{caT^4}{4\pi}\, b(\nu,T) \quad , \tag{4}$$

where a is the radiation constant. The advantages of using the reduced frequency distribution function are that the strong temperature dependence of thermal emission is factored out by the T^4 term, and that its frequency integral is independent of temperature,

$$\int_0^\infty d\nu\, b(\nu,T) = 1 \quad . \tag{5}$$

In slab geometry, the interaction of radiation with matter is expressed by the conservation law

$$\frac{\partial E_{mat}}{\partial t} = 2\pi \int_0^\infty d\nu \int_{-1}^{1} d\mu\, \sigma'_a[I - B(\nu,T)] + G \quad , \tag{6}$$

where E_{mat} is the energy per unit volume of the material and G is a volume source of energy. The change in energy of the material is related to the change

in temperature by its density times the specific heat, ρc_v, which may itself be a function of temperature

$$dE_{mat} = \rho c_v dT \quad . \tag{7}$$

In general, the resulting system of equations is non-linear with the material properties such as opacity and specific heat being represented in tabular form. For real problems of interest numerical solution has been our only viable approach.

3 The difference formulation

Noting that the solution to the transport equation approaches $B(\nu, T(x,t))$ in the limiting case of a thick system, and that the term $I - B$ occurs in both the transport equation and the equation for energy conservation, we define a difference intensity

$$D(\mathbf{x}, t; \nu; \mathbf{\Omega}) := I(\mathbf{x}, t; \nu; \mathbf{\Omega}) - B(\nu, T(\mathbf{x}, t)) \tag{8}$$

and, analogously, in slab geometry

$$D(x, t; \nu; \mu) := I(x, t; \nu; \mu) - B(\nu, T(x, t)) \quad . \tag{9}$$

We now subtract $(1/c)(\partial B/\partial t) + \mu(\partial B/\partial x)$ from both sides of Eq. (1),

$$\begin{aligned} \frac{1}{c}\frac{\partial D(x,t;\nu;\mu)}{\partial t} + \mu\frac{\partial D(x,t;\nu;\mu)}{\partial x} &= -\sigma'_a(\nu, T(x,t))D(x,t;\nu;\mu) \\ &\quad -\frac{1}{c}\frac{\partial B(\nu, T(x,t))}{\partial t} - \mu\frac{\partial B(\nu, T(x,t))}{\partial x} \quad , \end{aligned} \tag{10}$$

identifying the last two terms as sources for the transformed equation.

The interaction of radiation with matter is transformed to

$$\frac{\partial E_{mat}}{\partial t} = 2\pi \int_0^\infty d\nu \int_{-1}^{1} d\mu\, \sigma'_a D + G \quad . \tag{11}$$

Let us compare now Eq. (1) to Eq. (10). The propagation and absorption terms of the I field and the D field are the same. In contrast, the source term $\sigma'_a B$ has been traded for the space-time derivative of B. In a thick system with

smoothly varying temperatures, the new source terms as well as D are small. The transformed energy equation expressed in terms of the difference field, D, removes the stiff balance between emission and absorption.

An additional impact on numerical solutions is the fact that the emission term for the standard formulation contains a factor of σ_a', adding significant complexity for real materials that have a fine structure representing absorption lines. Because of this, it can be quite difficult to sample the emission spectrum without washing out this level of detail. In comparison, the source terms for the difference formulation are smooth and are accurately sampled using robust methods described in the Appendix. This lack of dependence of the source terms upon material properties makes implementing a code that treats spectral features accurately far less cumbersome, with spectral details appearing only in the absorption terms as particles are tracked and scored.

4 Symbolic Implicit Monte Carlo method

We have extended the Symbolic Implicit Monte Carlo (SIMC) method in order to develop a Monte Carlo solution for the difference formulation. Details of the SIMC method are described in [10] and [11]. One crucial component of SIMC is the factorization of the Planck function, $B = b(\nu, T)(caT^4/4\pi)$, in Eqs. (4) and (5). It allows an implicit treatment of the strongly varying T^4 term in the transport equation. The $b(\nu, T)$ term, with a frequency integral that is independent of the temperature, determines the frequency distribution of the sources.

In the discussion below, we will sketch the implementation of the SIMC method for the standard formulation as well as for the difference formulation, emphasizing their differences. Since our goal is to understand the basic advantage that the difference formulation offers in thick systems, we use an implementation without weight vectors in frequency space. In our Monte Carlo implementation of the two transport formulations we use a piecewise constant treatment of the material temperature, constant as a function of space within each zone and within each time step. As noted in the introduction, this treatment must be extended if we are to obtain the proper diffusion limit for zones that are optically thick.

In the standard formulation, the strength of thermal emission within a time step Δt in zone i, integrated over frequency, is approximated by

$$\Delta x_i \Delta t c a T_i^4(t_0 + \Delta t) < \sigma_a'(T_i(t_0)) > \quad , \tag{12}$$

where Δx_i is the volume of the zone, $T_i(t_0 + \Delta t)$ is the unknown temperature

of the zone at the end of the time step, $T_i(t_0)$ is the known temperature of the zone at the start of the time step, and $< \sigma_i'(T_i(t_0)) >$ is the Planck average of the absorption cross section given by,

$$< \sigma_a'(T_i(t_0)) > = \int_0^\infty d\nu \, \sigma_a'(T_i(t_0)) b(\nu, T_i(t_0)) \quad . \tag{13}$$

In the SIMC implementation, thermal emission is handled by emitting particles containing an unknown factor, $T_i^4(t_0 + \Delta t)$; the latter is solved for and substituted at the end of the time step. The source term is uniformly distributed within the zone, across the time step, and in the direction cosine, μ. The frequency distribution of thermal emission in the zone is given by

$$\frac{\sigma_i'(T_i(t_0)) b(\nu, T_i(t_0))}{< \sigma_i'(T_i(t_0)) >} \quad . \tag{14}$$

For a non-trivial cross section, the distribution function described above is constructed and tabulated for each zone at the start of each time step.

In the difference formulation the source terms are more complicated, but offer the advantage of independence from the detailed optical properties of the material. The first complication is that the source is not positive definite, the solution for the difference field itself only being bounded from below by $-B(\nu, T(x,t))$. There are two source components,

$$-\frac{1}{c}\frac{\partial B(\nu, T(x,t))}{\partial t} - \mu \frac{\partial B(\nu, T(x,t))}{\partial x} \quad , \tag{15}$$

each with different spatial and angular properties. With hindsight, we decompose the sources appropriately for the SIMC treatment

$$-\frac{1}{c}\frac{\partial B}{\partial t} - \mu \frac{\partial B}{\partial x} = \frac{\partial B}{\partial T^4}\left[-\frac{1}{c}\frac{\partial T^4(x,t)}{\partial t} - \mu \frac{\partial T^4(x,t)}{\partial x}\right] \quad . \tag{16}$$

We recognize that the frequency dependence of the emission is determined by $\partial B / \partial T^4$ only. We will use a discretized form of the derivative for our purposes. Accordingly, we define the distribution function

$$f[\nu, T_1, T_2] = \frac{T_1^4 \, b(\nu, T_1) - T_2^4 \, b(\nu, T_2)}{T_1^4 - T_2^4} \quad , \tag{17}$$

that has unit integral over frequency. The temperatures T_1 and T_2 are either the temperatures at the beginning and end of the time step, or are the temperatures on the left and right hand side of a zone interface. It yields the

reduced Planck distribution, $b(\nu, T)$, when one of the temperatures is zero. It must be treated with care when the difference in temperatures is small if a correct spectrum is to be obtained. We discuss this, along with our sampling techniques for $f[\nu, T_1, T_2]$, in the Appendix.

In finite difference form, the $\partial B/\partial t$ component of the source terms within a time step Δt is

$$\begin{aligned} & a\Delta x_i \left[T_i^4(t_0)b(\nu, T_i(t_0)) - T_i^4(t_0+\Delta t)b(\nu, T_i(t_0+\Delta t))\right] \\ & = a\Delta x_i f[\nu, T(t_0), T(t_0+\Delta t)][T_i^4(t_0) - T_i^4(t_0+\Delta t)] \quad . \end{aligned} \tag{18}$$

It is distributed uniformly in μ, spatially within the zone, and temporally across the time step. We do not have the temperature at the end of the time step available when frequency sampling is done, so an extrapolated value is used in $f[\nu, T(t_0), T(t_0+\Delta t)]$.

The $\partial B/\partial x$ component of the source is zero everywhere except on zone boundaries due to the piecewise constant treatment of the material temperature. The emission by this term within a time step Δt is

$$\mu \frac{ca}{2} \Delta t \left[T_l^4(t) b(\nu, T_l(t)) - T_r^4(t) b(\nu, T_r(t))\right] \quad , \tag{19}$$

where T_l refers to the temperature on the left side of an interface and T_r refers to the temperature on the right. Fixed temperature boundary conditions are handled by using the appropriately prescribed temperature. In finite difference form, it is approximated as

$$\mu \frac{ca}{2} \Delta t \left[T_l^4(t_0+\Delta t) - T_r^4(t_0+\Delta t)\right] f[\nu, T_l(t_0), T_r(t_0)] \quad . \tag{20}$$

Particles are sampled in balanced pairs traveling in the $\pm\mu$ directions with the frequency distribution function, $f[\nu, T_l, T_r]$, evaluated at the beginning of the time step. A value extrapolated to the end of the time step could be used. The T^4 "strength" terms are evaluated at the end of the time step in order to preserve stability.

The non-linear system to solve in order to perform the temperature update is obtained by integrating Eq. (6) for the standard formulation, or Eq. (11) for the difference formulation, taking advantage of Eq. (7) to relate the change in energy to the change in temperature. The scoring of thermally emitted particles yields a banded matrix in the space of zone indices where the bandwidth is controlled by $c\Delta t$, and also by the opacity because we removed particles

that had been attenuated to less than 10^{-6} times their birth weight. The non-linear system is solved by Newton - Raphson iteration after the Monte Carlo particles reach census. The actual value of $T_i^4(t_0 + \Delta t)$ is then substituted, thereby converting all census particles to known weights in order to prepare for the next time step. The basic scheme is the same for both the standard and the difference formulations. Only the details of the scoring function are different. In the standard formulation, the unknown factor is $T_i^4(t_0 + \Delta t)$. In the difference formulation, the unknown factors are $(T_i^4(t_0) - T_i^4(t_0 + \Delta t))$, and $(T_l^4(t_0 + \Delta t) - T_r^4(t_0 + \Delta t))$, for particles produced by the $\partial B/\partial t$ and the $\partial B/\partial x$ source terms, respectively. [1]

5 Test problems

A variety of test problems have been examined in order to evaluate the computational efficiency and accuracy of the difference formulation, employing the SIMC Monte Carlo method described above. Our goal is to analyze some simple situations that indicate the potential impact of the difference formulation in more complex physics environments. The key issues are accuracy and efficiency for both thick and thin media – specifically the frequent occurrence of media which are thick at one frequency while being thin at others. In addition to comparing the Monte Carlo solution of the two formulations of transport, we compare them to semi-analytic solutions where they are available.

5.1 Behavior of a finite slab heated from the outside

The most basic test of a thermal transport algorithm is whether it correctly approaches the steady state solution for a finite slab immersed in a heat bath with different temperatures on either side. At the coarsest level, in thick media, the steady state solution of the material temperature, raised to the fourth power, is a straight line when plotted as a function of optical depth. Deviations from a straight line are indicative of boundary layers when they occur within a mean free path or so of a surface, but otherwise they indicate serious problems in the numerical solution. Teleportation errors result in a wrong slope and cause curvature in the interior solution [14]; this is the reason why we limit zone thickness to one mean free path for our piecewise constant treatment of the material temperature.

[1] In the $\partial B/\partial t$ term, the temperature is handled in the form $(T_i^4(t_0) - T_i^4(t_0 + \Delta t))$, both to simplify the code and to avoid the noise and possible numerical difficulties associated with two independent particle weights when tracking Monte Carlo particles.

The time dependent approach to steady state offers the opportunity to check the correctness of the implementation of interior source terms as well as initial and boundary conditions. That the steady-state temperature is independent of time step, reflecting implicit behavior of the time integration, can also be checked. When the spectrum of the radiation field is examined, even for a gray opacity, the correctness of the frequency sampling algorithm can be checked. Agreement between the standard and difference formulation is non-trivial due to the different nature of their source terms. A detailed description of all the checks described above is beyond the scope of this paper, but they have been carried out.

In the presentation of our computational results below, we provide a clear demonstration of rigorous agreement between the two formulations for transport, in terms of their approach to steady state, along with a measure of the increase in computational efficiency for the difference formulation. The magnitude of this increase in computational efficiency, in the form of greatly reduced Monte Carlo noise as the optical thickness of the problem is increased, is somewhat surprising even to the authors who were prospecting for it.

In the first set of simulations we consider a finite slab heated from the left side, with an open boundary on the right, allowing the radiation flowing through the slab to enter free space. The slab is composed of a uniform, static material having a frequency-independent (gray) opacity. We calculate the time dependence of the temperature and of the radiation field after a 1 keV black-body source on the left side of the slab is turned on at time $t = 0$. (1 keV $\approx$ 1.2 10^7 °K.)

During the time dependent execution of the problem, a thermal wave, also known as a Marshak wave, sweeps the problem domain, and the solution then approaches steady state. Under conditions where the Monte Carlo portion of the code dominates execution time, we compare the solutions provided by the two formulations. The relative noise for identical problem run times provides a measure of computational efficiency.

For four instances of this problem, the slab is composed of a uniform material having a frequency independent (gray) opacity of 0.1, 1, 10, and 100 mean free paths per cm, respectively. The specific heat of the material is a constant 0.1 jerk/(keV cm^3), where jerk is an energy unit (1 jerk = 10^{16} ergs), and temperature is measured in energy units of kT = 1 keV. The slab is initially at a temperature of 0.01 keV, with the radiation field being a Planckian in equilibrium with this temperature. The slab is 10 cm thick, so the four opacities correspond to total optical depths of 1, 10, 100 and 1000 mean free paths. All four problems used a time step of 0.2 sh, where 1 sh = 10^{-8} sec. The problems 1 and 10 mean free paths thick were run to 20 sh to equilibrate. The problem 100 mean free paths thick was run to 40 sh in order to approach

steady state. The problem 1000 mean free paths moved very slowly due to the diffusive nature of the solution, requiring 320 sh in order to suitably approach steady state. The problems 1 and 10 mean free paths thick employed 20 zones, while the thicker problems employed zones one mean free path thick in order to prevent teleportation error from influencing the results and to prevent anomalous performance results for the difference formulation. Zones of equal thickness were used everywhere. Geometric zoning has a role in reducing computational cost only if a piecewise linear treatment of material properties is available to keep teleportation error under control [19].

A time step size of 0.2 sh is enough time for a photon to travel 6 times the thickness of the slab, reflecting on the stability of the method. Relaxing the need for implicit treatment of the source terms was one of the hopes of the authors, given that implicit treatment requires the solution of a non-linear system of equations for each time step. Our experiences in this regard, documented in [22], were made even more difficult by the T^4 term for thermal emission. As a result, explicit treatment of the $\partial B/\partial x$ source terms was abandoned. It may be worth revisiting in more complex physics applications where the time step size is limited for reasons outside of transport physics.

Note that the Monte Carlo solution for the two transport formulations have entirely different requirements for spatial importance sampling if uniform statistical noise, as a function of position, is to be obtained. In the standard formulation most of the computational effort is spent computing the balance between emission and absorption that produces the local equilibrium blackbody field. As a result, a scheme that samples particles with uniform density in space produces a relatively flat statistical noise profile across the slab. During each time step, the number of source particles born in each zone is proportional to the thickness of the zone. The statistical properties of the Monte Carlo solution for the difference formulation are in sharp contrast to this. For thicker problems the statistical noise for the difference formulation is small near the hot side and increases rapidly towards the cold boundary. Suitable importance sampling flattens out this growth in noise. An exposition of this topic is beyond the scope of this paper. In our tests we sampled source particles uniformly in space.

In the examples shown in this paper, the unit of source sampling for the difference formulation is one $\partial B/\partial t$ particle and one $\partial B/\partial x$ particle pair, for each zone or zone interface, respectively. We have not attempted to tune the ratio between $\partial B/\partial t$ and $\partial B/\partial x$ source particles, nor have we attempted to tune the relative importance of source sampling across the volume of the problem. In the standard formulation the unit of source sampling is one thermally emitted particle per zone.

In Figure 1 (a) we show the steady-state solution for the material temperature

as a function of position in the slab that is one mean free path thick. The average of 100 randomly seeded runs using the standard formulation, and the difference formulation, is shown. The two formulations are in good agreement. The standard deviation of the results for the standard formulation as well as for the difference formulation, both multiplied by 400, are plotted. The number of Monte Carlo source particles was selected to produce equal run times for the two formulations and was high enough that the cost of Monte Carlo transport dominated execution time. The relative performance of the methods is then the ratio of the squares of the their standard deviations. There is a small advantage in favor of the difference formulation, except at the very right hand side of the slab. Note that the optical thickness of each zone is only 0.05 optical depths.

In Figure 1 (b) we show the results for a slab that is 10 mean free paths thick. Again, we obtain excellent agreement between the two formulations, comparing the equilibrium material temperature. In order to display the standard deviation of the temperature for the two formulations on the same plot, we apply a scale factor of 100 for the standard formulation and 1000 for the difference formulation. The trend of growth for the standard deviation for the difference formulation, as the temperature gradient increases in the slab from left to right, is becoming apparent.

In Figure 1 (c) we show the results for a slab that is 100 mean free paths thick. There are 100 zones in this problem in order to minimize teleportation error, with every fifth point plotted using a symbol. The other points are included in the solid lines drawn. The growth in noise for the standard formulation is now becoming visible in the plot. We apply a scale factor of 20 to see the standard deviation for the standard formulation. The growth of the standard deviation for the difference formulation as one traverses the slab from left to right is now quite clear, but the overall computational advantage for the difference formulation has increased with optical depth.

In Figure 1 (d) we show the results for a slab that is 1000 mean free paths thick. There are 1000 zones in this problem, a requirement to avoid significant teleportation error, with every 50'th zone plotted using a symbol. The disagreement between the two formulations appearing towards the left side of the slab are due to statistical fluctuations in the standard formulation. The computational advantage of the difference formulation has continued to increase with opacity.

The reader may note that the results for the difference formulation have the appearance of smooth curves, regardless of the optical thickness of the problem. The $1/\sqrt{N}$ noise behavior that is typical of a Monte Carlo solution is present, it is just that the amplitude of the noise is too small to resolve in the figure for the cases we have illustrated.

Evidence of the scaling behavior of the computational advantage of the difference formulation is shown in Figure 2. The figure illustrates the computational advantage of the difference formulation when calculating the material temperature, as a function of position, for four optical thicknesses. The computational advantage scales roughly as the square of the optical depth of the problem.

In Figure 3 we show the penetration of a thermal wave into a slab 1000 mean free paths thick at 40 sh, for a single problem run with the same parameters as in Figure 1 (d). The solution shown is fully converged as a function of time step and zone size. This figure visibly illustrates the gains that the difference formulation provides.

5.2 Comparison to analytic diffusion solution for a linearized problem

In order to check the correctness of our numerical implementation, we have compared our results with the diffusion solution appearing in [21]. This solution requires that the material energy take the form

$$E_{mat} = \frac{\alpha T^4}{4} \tag{21}$$

or, equivalently, that the specific heat take the form

$$\frac{\partial E_{mat}}{\partial T} = \alpha T^3 \quad , \tag{22}$$

where α is a specified constant. This form for the material energy removes the non-linearity, T^4, that otherwise prevents an analytic solution. The resulting analytic solution can then be used to check for the correct convergent behavior in our numerical simulation. The behavior of the specific heat at $T = 0$, however, makes the numerical calculation quite fragile unless the code itself is transformed to handle things in the linearized form. To some extent, this defeats the purpose of checking the original code, much of which had to be modified to accommodate the linearized form.

For this problem α and the absorption cross section were chosen so that the values in the tables of analytical results appearing in [21] could be used directly. In Figure 4 we plot the material temperature produced by our Monte Carlo solution of the standard and difference formulations, along with data from Su and Olson's analytical solution corresponding to a late time, their $\tau = 10$. We obtain good agreement where analytical data are available. This is expected because for $\tau = 10$ the diffusion approximation assumed by Su and Olson is valid. In Figure 5 we plot the material temperature for the same

problem along with data from Su and Olson's analytical solution for $\tau = .01$. Not surprisingly, there is sharp disagreement between the diffusion solution and the fully overlapped and converged Monte Carlo transport solutions for the standard and the difference formulations. Here the fundamental limitation is the speed of light; it is fully respected by the transport solution but ignored by the diffusion solution, unless ad-hoc corrections are used.

5.3 Time dependent Marshak wave problem, with a non-trivial opacity

Our Monte Carlo solutions of the standard and difference formulations of transport fully implement the details of the thermal frequency spectrum; the spectral properties of the derivative sources make the agreement between the two formulations non-trivial even in the case of a gray opacity. Once the spectral sampling of the source terms in the difference formulation is done correctly, as described in the Appendix, there is no more to be done for the correct treatment of a frequency dependent opacity in the difference formulation other than to use the correct absorption cross section for the given Monte Carlo particle. The accuracy of the treatment of the frequency dependent cross section is as good as the cross section itself.

The emission term for the standard formulation, on the other hand, appears as $\sigma'_a B$. In the most general case, it must be numerically integrated across the frequency group structure in each zone at the start of each time step. This requirement provides another place where numerical errors must be controlled in the implementation of the standard formulation.

We now turn to a relatively simple frequency dependent opacity: one that is 1000 mean free paths for the slab for frequencies below 1 keV and 10 mean free paths for the slab for frequencies above 1 keV. This corresponds, roughly, to the precipitous drop in opacity as a function of frequency that can occur in real materials. The portion of the emitted spectrum below 1 keV is strongly reabsorbed, while the portion of the emitted spectrum above 1 keV encounters a lower opacity and transports freely. This is a difficult non-linear problem because, as the trapped radiation heats the material, the Planckian emission spectrum moves towards higher frequencies where radiation flows freely.

In Figure 6 we show the material temperature for one instance of this problem at $t = 1$sh a time where the thermal wave is still propagating through the slab. As before, the standard formulation is the one exhibiting a high level of statistical noise. Note, however, that this noise disappears in the "foot" of the advancing thermal wave. This feature is produced by high-frequency photons that encounter a lower material opacity.

6 Summary and conclusions

The Symbolic Implicit Monte Carlo method (SIMC) [10] is an attractive framework for the calculation of radiation transport in complex media and geometries; it provides a basis for accurate and stable numerical schemes [11] [12]. In this paper we have demonstrated that the difference formulation [16] is eminently suitable for numerical calculations of radiation transport in LTE, employing the SIMC technique.

Our theoretical expectations were that the traditional formulation would be better for thin media, while the difference formulation would be advantageous in thick media. We have demonstrated that the difference formulation, when employing the SIMC technique, offers significant noise reduction for thick systems, with its computational advantage scaling like the square of the opacity. The expected cross-over *vis-a-vis* the standard formulation occurs only for very thin systems, thin enough that the difference formulation might become a panacea for the Monte Carlo treatment of thermal radiation transport in practical problems.

The character of the source terms is very different in the traditional and the difference formulations: thermal emission in the former is replaced by derivative source terms in the latter. Therefore a key issue for the accuracy and stability of the difference formulation is the successful treatment of the derivative source terms. We have developed efficient, accurate analytic techniques for sampling the frequency spectrum of the source terms for the difference formulation. Frequency sampling in the difference formulation depends only on the space and time derivative of the material temperature, not on its optical properties. This offers a significant advantage for problems with complicated material optical properties. The value of this reduction in code complexity became clear when we implemented the test problem with the step in opacity. Although the test problems we presented were simple in order to clearly identify the advantages of the difference formulation, extensions to more complex situations do not present conceptual difficulties.

The computational gain for the difference formulation demonstrated in this paper is for the Monte Carlo portion of the problem. In order to obtain implicit treatment of the source terms, the SIMC technique requires the solution of a non-linear system of equations in order to perform the temperature update at the end of the time step. The cost of this can become significant when the number of zones in the problem is large. We used band-limited Gaussian elimination in our numerical work on problems with as many as 1000 zones. The bandwidth was limited both by the time step size and by the death of Monte Carlo particles when they became too small, relative to their birth weight. Multi-dimensional problems with significantly larger numbers of zones

will pose a challenge, requiring the use of suitable iterative solution techniques. Nonetheless, we believe that the demonstrated noise reduction in thick systems will be worth the effort involved.

In our numerical evaluation of the difference formulation, we have employed a piecewise constant discretization for the material temperature. Due to teleportation effects, this discretization does not provide the correct diffusion limit for zone sizes that are large compared to the mean free path of a photon. A piecewise linear treatment of the material temperature is required to remove this defect [19]. In order to obtain a more accurate solution, both the time discretization and the treatment of the frequency spectrum of the emitted photons will have to be improved. These issues will be addressed in future work.

Our test problems have been relative simple, suitable as the first numerical tests for the difference formulation for thermal radiation transport. In our presented results it is clear that the importance sampling requirements for the difference formulation are quite different than those for the standard one. It is also the case that improvements such as weight vectors in frequency space and deterministic handling of the spectral output from the interface adjoining free space have a significant impact on noise when spectral information associated with the photon field is desired. The details of these enhancements, along with their relative value, are dependent upon the exact nature of the problems being run and the computational results that are desired. They are beyond the scope of this paper.

Finally, we note that our work may open the door to significant improvements in the numerical treatment of more general transport problems and methods. We can envisage application to scattering atmospheres, Comptonization, [2] etc. Although this paper provides no obvious lessons for deterministic methods, these might also benefit from the smallness of the source terms appearing in the difference formulation, for thick systems.

7 Appendix: sampling the frequency probability density function

The frequency probability density function (p.d.f.) was given previously in Eq. (17) as a function of frequency ν and two temperatures, T_1 and T_2:

$$f\left[\nu, T_1, T_2\right] = \frac{b\left(\nu, T_1\right) T_1^4 - b\left(\nu, T_2\right) T_2^4}{\left(T_1^4 - T_2^4\right)} \tag{23}$$

Sampling a frequency from this distribution function is not straightforward because there are two limiting cases to deal with. The first occurs when one

of the temperatures is zero (or is a vacuum interface). In this event, the p.d.f. turns into a Planckian as normally sampled in IMC and SIMC [20]. The other limiting situation is when the temperatures are very close together. There, the limit of the p.d.f. as T_2 approaches T_1 must be used, which returns us to the original derivative:

$$\lim_{T_1 \to T_2} \frac{b(\nu, T_1) T_1^4 - b(\nu, T_2) T_2^4}{(T_1^4 - T_2^4)} = \frac{4\pi}{ca} \frac{\partial B(\nu, T)}{\partial T^4}. \tag{24}$$

This may be sampled by expanding B and defining $x = h\nu/kT$ to get a unitless cumulative density function (c.d.f.) for x:

$$\begin{aligned} c.d.f. &= \int_0^{\nu} \frac{4\pi}{ca} \frac{\partial B(\nu', T)}{\partial T^4} d\nu' \\ &= \int_0^{\nu} \frac{15}{4\pi^4} \frac{e^{h\nu'/kT} h^5 \nu'^4}{\left(e^{h\nu'/kT} - 1\right)^2 k^5 T^5} d\nu' \\ &= \int_0^{x} \frac{15}{4\pi^4} \frac{x'^4 e^{-x'}}{\left(1 - e^{-x'}\right)^2} dx' \end{aligned} \tag{25}$$

Multiplying and dividing the integrand by $(1 + e^{-x}/x^2)$ gives a probability distribution function (p.d.f.) of the form

$$p.d.f.(x) = [\pi_1 f_1(x) + \pi_2 f_2(x)]\, h(x); \qquad x \geq 0 \tag{26}$$

where $\pi_1 + \pi_2 = 1$ and $\int_0^{\infty} f_i(x)\, dx = 1$. It can be verified that $\pi_1 = 96/97$, $\pi_2 = 1/97$, $f_1 = (1/24)x^4 e^{-x}$, $f_2 = 4x^2 e^{-2x}$, and
$h = [1455x^2]/[16\pi^4 \left(1 - e^{-x}\right)^2 (x^2 + e^{-x})]$.

This may be sampled by using the rejection technique with the comparison function being this function with $h(x) = h_{\max}$. Then f_1 is sampled with a probability of π_1 and f_2 is sampled otherwise. The sample is kept if a random number is less than $h(x_i)/h_{\max}$.

Finally, in the most general case we investigated two options, the first of which is to develop a table lookup method. The reduced Planckian, $b(x)$, is numerically integrated and fitted with a spline. Then a Newton-Raphson method is used to find the frequency for this c.d.f.

The second method employs a rejection technique by expanding b and defining $C = T_{\min}/T_{\max}$ and $x = h\nu/kT_{\max}$ to get a c.d.f.:

$$\int \frac{x^3}{1-C^4}\left(\frac{1}{e^x-1}-\frac{1}{e^{x/C}-1}\right)dx \tag{27}$$

There is a comparison function that can be used for rejection which is defined as

$$f(x) = x^2 e^{-1.5x} + x^3 e^{-ax};\ C = T_{\min}/T_{\max};\ a = 1-0.1C \tag{28}$$

The frequency may be then be sampled with the following simple algorithm where r's represent random numbers from 0 to 1:

(1) If $r_1 < 1/\left[1-\left(3\cdot 1.5^3\right)/a^4\right]$ then goto (2) else goto (3)
(2) Sample $x^2e^{-1.5x}$. $x = \ln\left(r_3r_4r_5\right)/1.5$. Goto (4).
(3) Sample x^3e^{-ax}. $x = \ln\left(r_3r_4r_5\right)/a$.
(4) If $f(x)\cdot r_2 > x^3\left[\left(e^x-1\right)^{-1}-\left(e^{x/C}-1\right)^{-1}\right]/\left(1-C^4\right)$ then goto (1).
(5) Sampled frequency is $xT_{\max}$.

Speed and accuracy were investigated on four different machines for a variety of C values (ratio of low to high temperature). The accuracy of the Planckian, table lookup and general rejection method appeared to be about the same for $C \leq 0.01$. Similarly, the accuracy of $\partial B/\partial T^4$ limit, table lookup and general rejection method were about the same for $C \geq 0.99$.

Timing depended upon the computer employed, but there were general trends. Each method was sampled 100 million times on each machine for different values of C. For C below 0.1, the fastest method was the Planckian. The general rejection method was 15% slower and the table lookup was about twice as slow. For C above 0.9, the fastest method was the $\partial B/\partial T^4$ limit. The general rejection method using Eq. (27) was about the same speed while the table lookup was about four times slower.

In summary, we use the Planckian method for $C \leq 0.01$, $\partial B/\partial T^4$ limit method for $C \geq 0.99$ and the general rejection method using Eq. (27) otherwise.

Acknowledgments

The authors would like to thank Bret Beck for contributing the rejection technique that sampled the two temperature frequency distribution function.

References

[1] D. Mihalas, Stellar Atmospheres, (San Francisco; Freeman), pp 64 - 71, 1978.

[2] John I. Castor, *Lectures on Radiation Hydrodynamics*, UCRL-JC-134209, 2000.

[3] Mihalas, D. and Mihalas, B. W., *Foundations of Radiation Hydrodynamics*, (New York: Oxford University Press), 1984.

[4] Pomraning, G. C. *The Equations of Radiation Hydrodynamics*, (Oxford: Pergamon), 1973.

[5] J.A. Fleck, Jr. and J.D. Cummings, *An implicit Monte Carlo scheme for calculating time and frequency dependent radiation transport*, J. Comput. Phys. **8**, 313 (1971).

[6] Larsen, E. W., Pomraning, G. C. and Badham, V. C. *Asymptotic analysis of radiative-transfer problems*, J. Quant. Spectr. Rad. Transfer **29**, 285 (1983).

[7] G.C. Pomraning, *Flux Limiters and Eddington Factors*, J. Quant. Spectr. Rad. Transfer **27**, 517-530.

[8] R.E. Marshak, *Note on the Spherical Harmonic Method As Applied to the Milne Problem for a Sphere*, Phys Rev 1947;71:443-6

[9] J.C. Mark, *The spherical harmonic method*, Technical Report, CRT-340, Atomic Energy of Canada, Ltd., Ontario, 1947.

[10] E.D. Brooks III, *Symbolic Implicit Monte Carlo*, J. Comput. Phys. **82**, 433 (1986).

[11] T. N'kaoua, *Solution of the nonlinear radiative transfer equations by a fully implicit matrix Monte Carlo method coupled with the Rosseland diffusion equation via domain decomposition*, SIAM J. Sci. Stat. Comput. **12**, 505 (1991).

[12] Densmore J.D., Larsen E. W., *Asymptotic Equilibrium Diffusion Analysis of Time-Dependent Monte Carlo Methods for Grey Radiative Transfer*, Journal of Computational Physics (in press), Los Alamos National Laboratory preprint LA-UR-03-9164.

[13] L.L. Carter and C.A. Forest, *Nonlinear radiation transport simulation with an implicit Monte Carlo method, LA-5038, Low Alamos National Laboratory*, 1973 (unpublished).

[14] M. S. McKinley, E. D. Brooks, and A. Szoke, *Comparison of Implicit and Symbolic Implicit Monte Carlo Line Transport with Frequency Weight Vector Extension*, J. Comp. Physics, 189, 330-349 (2003).

[15] J.A.Fleck and E.H.Canfield, *Random Walk Procedure For Improving The Computational Efficiency Of The Implicit Monte Carlo Method For Nonlinear Radiation Transport*, J. Comp. Physics, 54, 508-523 (1984).

[16] A. Szőke, E.D. Brooks III, *The transport equation in optically thick media*, J. Quant. Spectr. Rad. Transfer (in press), UCRL-JC-152828, Lawrence Livermore National Laboratory, (2003).

[17] J.E. Morel, T.A. Wareing, and K. Smith, *A linear-discontinuous spatial differencing scheme for S_N radiative transfer calculations*, J. Comput. Phys. **128**, 445 (1996).

[18] M.L. Adams and P.F. Nowak, *Asymptotic analysis of a computational method for time- and frequency-dependent radiative transfer*, J. Comput. Phys. **146**, 366 (1998).

[19] Clouet, J.-F. and Samba, G. *Asymptotic diffusion limit of the symbolic Monte-Carlo method for the transport equation* J. Comput. Phys. **195**, 293 (2004).

[20] C. Barnett and E. Canfield, *Sampling a random variable distributed according to Planck's law*, Lawrence Livermore National Laboratory, UCRL-ID-125393 (1970) (unpublished).

[21] B. Su and G.L. Olson, *Benchmark results for the non-equilibrium marshak diffusion problem*, J. Quant. Spectr. Rad. Transfer **56**, 337-351 (1996).

[22] Frank Daffin, et al., *An Evaluation of the Difference Formulation for the Transport of Atomic Lines*, in preparation for submission to J. Comput. Phys.

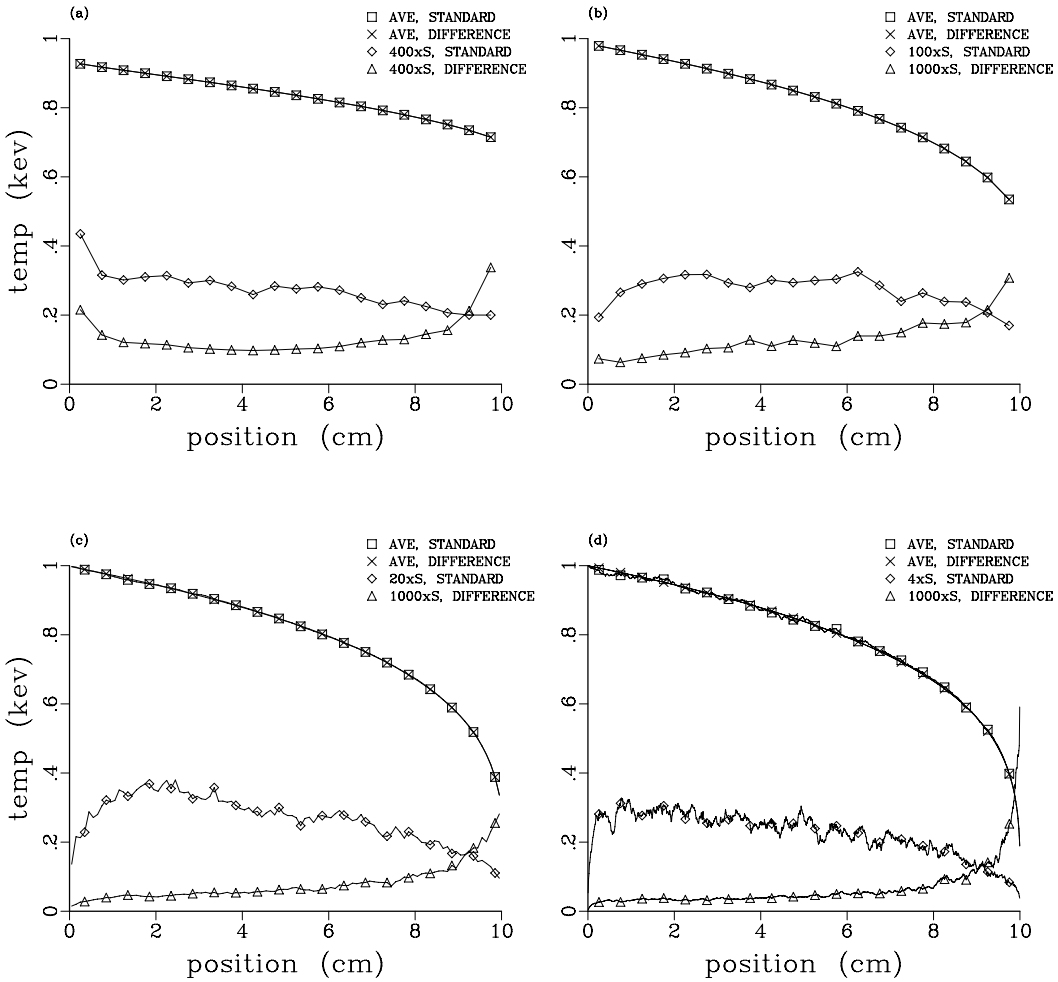

Fig. 1. Temperature distribution in a slab in steady state. The slab is heated from the left by a 1 keV black body, and it radiates freely on the right. The total optical depth (OD) of the slab is 1 in (a), 10 in (b), 100 in (c) and 1000 in (d). The standard deviation of the standard formulation is denoted by diamonds and that of the difference formulation by triangles. Note the change in their relative scale with optical depth. The noise in the standard SIMC Monte Carlo increases dramatically with optical depth, while in the difference formulation it does not.

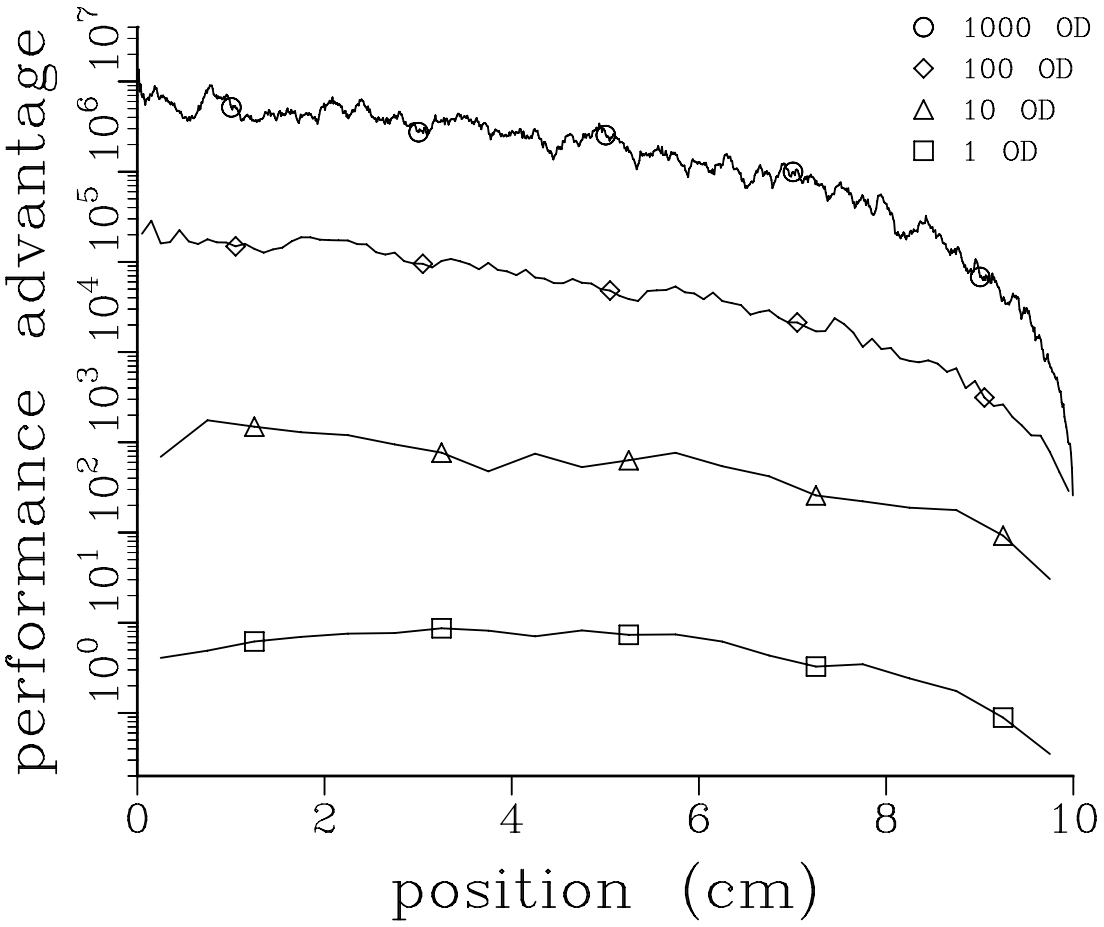

Fig. 2. The relative advantage of the difference formulation compared to standard SIMC, plotted as a function of position for various optical depths of the slab. The performance advantage increases almost quadratically with total optical depth. In the 1 OD case, each zone is only 1/20 OD thick, nevertheless, the difference formulation is almost as good as the standard one. There is a sharp decrease in advantage where the temperature gradient is large. This could easily have been remedied by importance sampling.

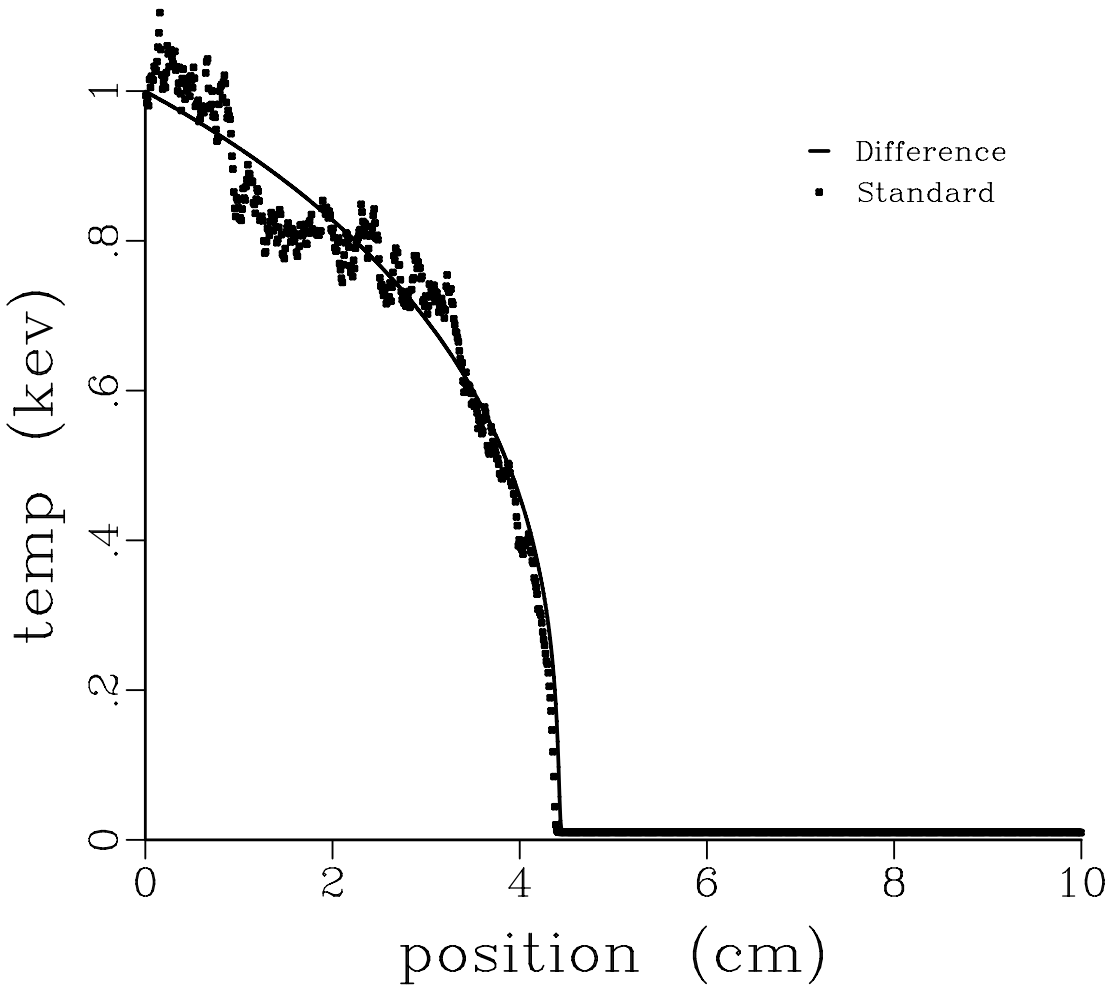

Fig. 3. Thermal wave (Marshak wave) penetrating a uniform, gray slab of 1000 OD at an early time, 40 sh. The standard formulation gives a noisy temperature profile whereas that of the difference formulation is many orders of magnitude smoother. As seen in Fig. 1, both calculations converge to the same temperature distribution in steady state. The slight difference in the position of the leading edge is a statistical fluctuation for the standard formulation.

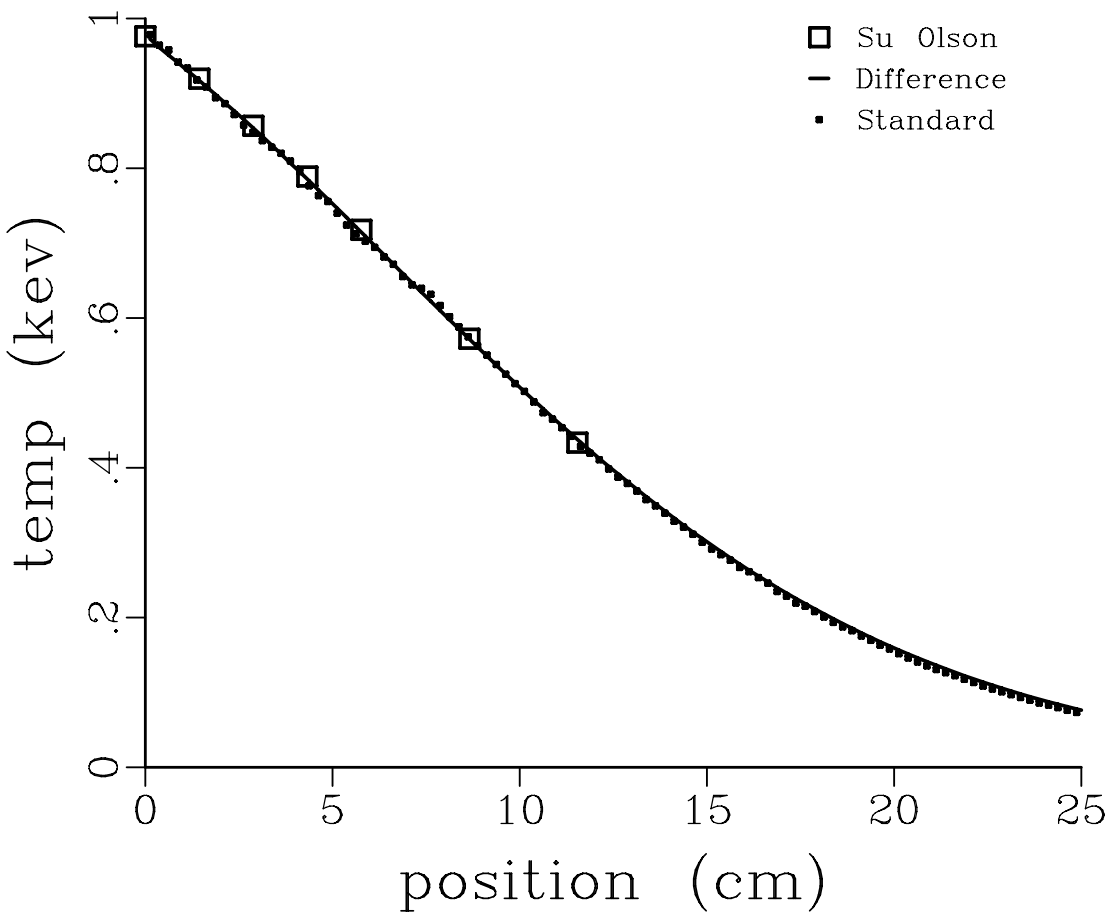

Fig. 4. Temperature distribution in the Su & Olson problem [21] at a late time $\tau = 10$. There is excellent agreement of the calculations with analytic results.

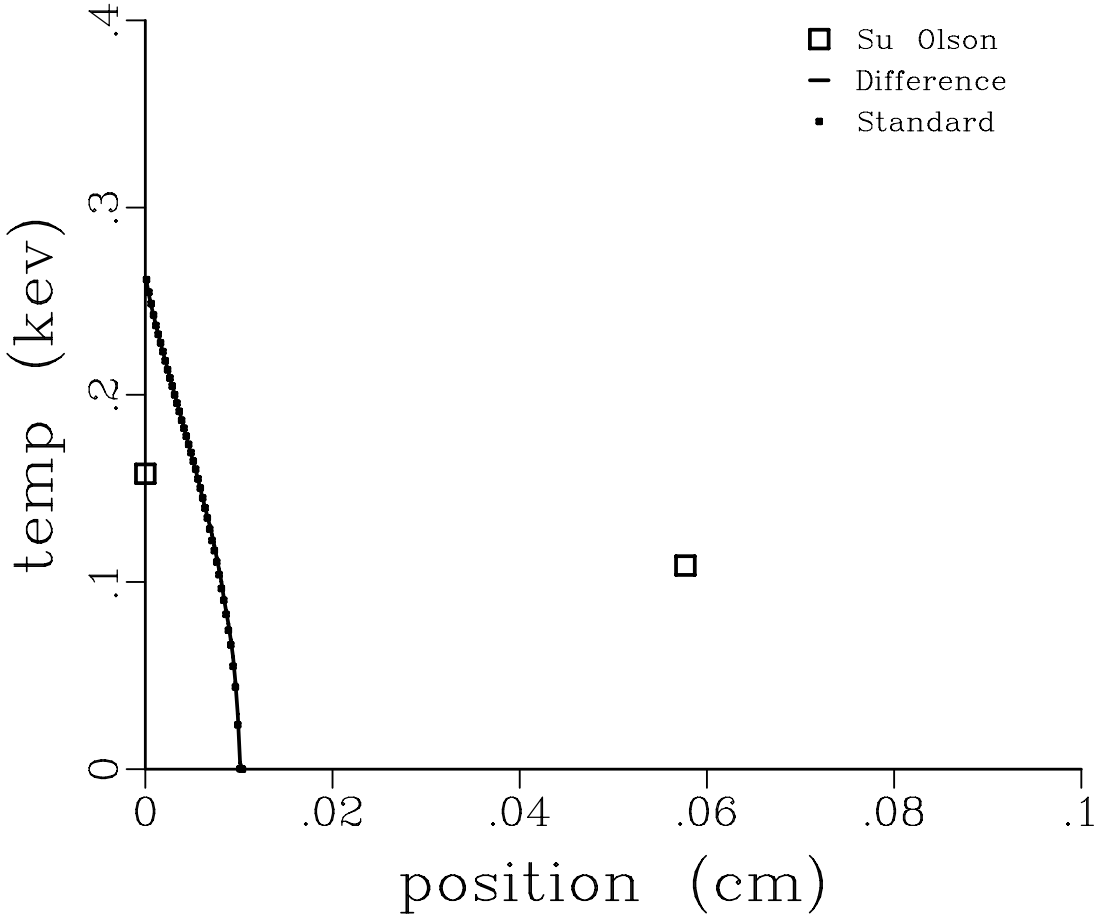

Fig. 5. Temperature distribution in the Su & Olson problem [21] at an early time $\tau = 0.01$. The transport solution is limited by the speed of light, that is 1 in those units. Note that there is no significant spreading of the radiation front at the leading edge of the thermal wave.

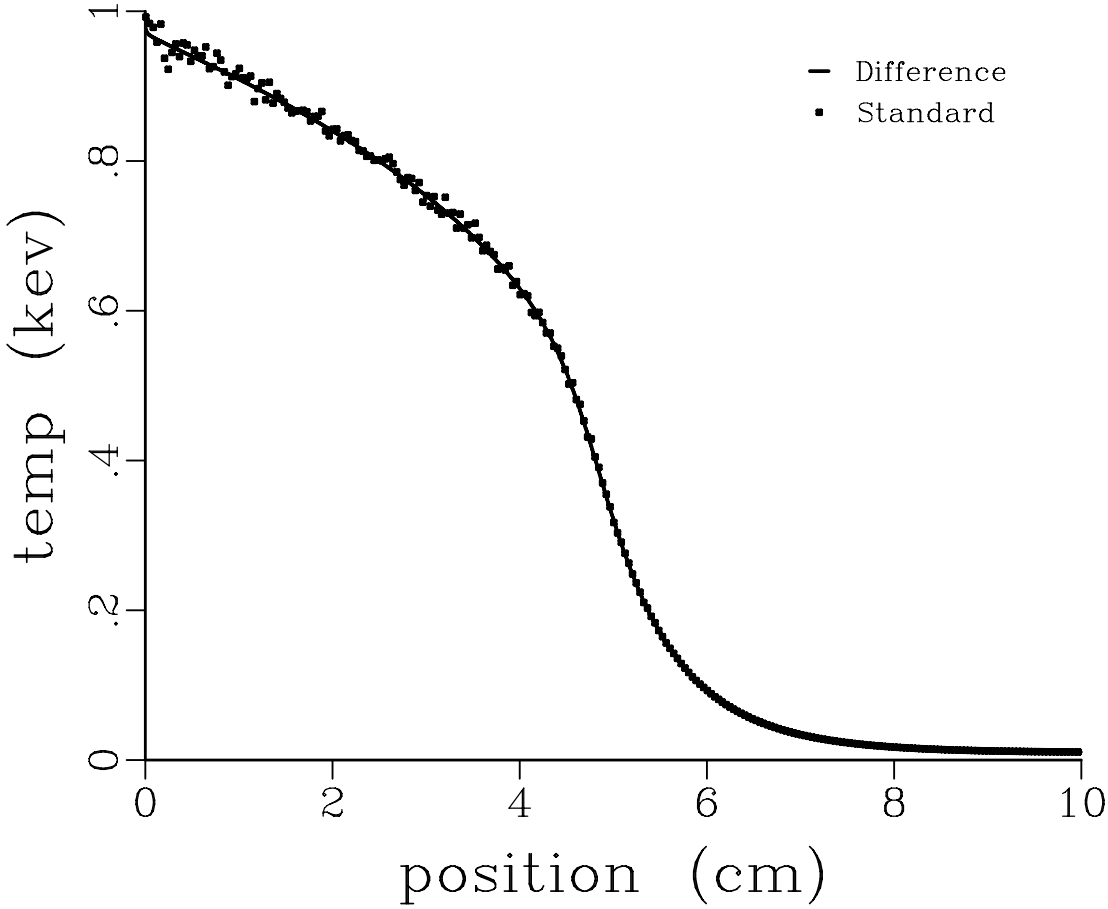

Fig. 6. Thermal wave penetrating a uniform slab with a non-trivial opacity. A 1 keV black-body source is turned on at $t = 0$, the temperature profile is shown at $t = 1\,\mathrm{sh}$. The opacity is constant (high) for frequencies below 1 keV and again constant (but low) for frequencies above 1 keV. At 1 keV the opacity of the material drops by a factor of 100. The long "foot" of the temperature stems from high frequency photons that penetrate deeply.

University of California
Lawrence Livermore National Laboratory
Technical Information Department
Livermore, CA 94551